Journal of Biomolecular NMR, **22:** 57–64, 2002.
KLUWER/ESCOM

Position of residues in transmembrane peptides with respect to the lipid bilayer: A combined lipid NOEs and water chemical exchange approach in phospholipid bicelles

Kerney Jebrell Glover, Jennifer A. Whiles, Regitze R. Vold & Giuseppe Melacini*
Department of Chemistry and Biochemistry, University of California, San Diego, 9500 Gilman Dr., La Jolla, CA 92093-0314, U.S.A.

Received 3 October 2001; Accepted 1 November 2001

Key words: circular dichroism, fluorescence, NMR, peptide-lipid NOEs, water chemical exchange

Abstract

The model transmembrane peptide P16 (Ac-KKGLLLALLLLALLLALLLKKA-NH_2) was incorporated into small unaligned phospholipid bicelles, which provide a 'native-like' lipid bilayer compatible with high-resolution solution NMR techniques. Using amide-water chemical exchange and amide-lipid cross-relaxation measurements, the interactions between P16 and bicelles were investigated. Distinctive intermolecular NOE patterns observed in band-selective 2D-NOESY spectra of bicellar solutions with several lipid deuteration schemes indicated that P16 is preferentially interacting with the 'bilayered' region of the bicelle rather than with the rim. Furthermore, when amide-lipid NOEs were combined with amide-water chemical exchange cross-peaks of selectively ^{15}N-labeled P16 peptides, valuable information was obtained about the position of selected residues relative to the membrane-water interface. Specifically, three main classes were identified. Class I residues lie outside the bilayer and show amide-water exchange cross-peaks but no amide-lipid NOEs. Class II residues reside in the bilayer-water interface and show both amide-water exchange cross-peaks and amide-lipid NOEs. Class III residues are embedded within the hydrophobic core of the membrane and show no amide-water exchange cross-peaks but strong amide-lipid NOEs.

Introduction

Transmembrane domains are involved in a variety of cellular processes including receptor dimerization, channel formation, and signaling (Arora et al., 2001; MacKenzie et al., 1997; Mumm and Kopan, 2000). These functions depend on specific interactions between a transmembrane domain and the lipid bilayer. Particularly, the secondary and tertiary structure of a transmembrane domain, embedded in a membrane, is largely determined by the lipid bilayer (Cross and Opella, 1994; Opella, 1997).

The lack of 'bilayered' membrane mimetics with sufficiently fast reorientation rates has limited high resolution solution NMR studies of transmembrane domains to micellar solutions (Kallick, 1993; Losonczi et al., 2000; Williams et al., 1996). However, the interpretation of the details of the interactions between the polypeptide and the lipid can not be clearly discerned in micelles due to their curvature and lack of a true bilayer. On the other hand, small unaligned phospholipid bicelles are uniquely suited to examine peptide-lipid interactions due to their 'bilayer' characteristics and their compatibility with high-resolution solution NMR techniques (Glover et al., 2001a,b; Vold et al., 1997; Whiles et al., 2001).

A bicelle is a discoidal lipid aggregate comprised of long chain phospholipid and a detergent. The long chain phospholipid forms a 'native-like' planar bilayer in the center, while the detergent is localized at the rim where it shields the long chain lipid tails from water (Ram and Prestegard, 1988; Sanders et al., 1994). The rim can be comprised of a short chain phospholipid such as dihexanoylphos-

*To whom correspondence should be addressed. E-mail: gm@chem.ucsd.edu

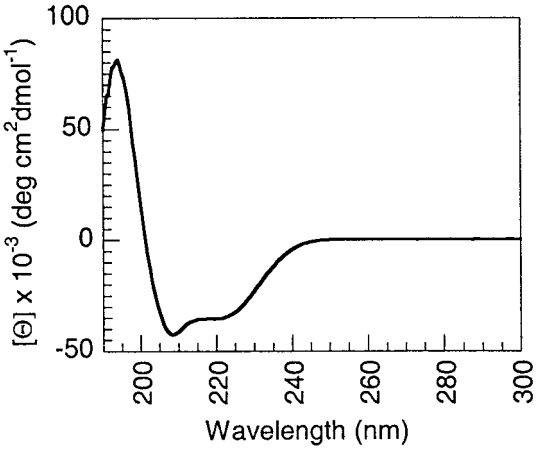

Figure 1. Circular Dichroism spectra of P16 in unaligned bicelles.

phatidylcholine (DHPC) or a bile salt derivative such as 3-(cholamidopropyl)dimethylammonio-2-hydroxy-1-propane-sulfonate (CHAPSO) (Sanders and Prestegard, 1990; Sanders et al., 1993; Sanders and Schwonek, 1992), while dimyristoylphosphocholine (DMPC), dilaurylphosphocholine, or dipalmitoylphosphocholine can be used for the planar region depending on the desired bilayer thickness (Czerski and Sanders, 2000). Moreover, the charge characteristics of the planar region can be varied by incorporating lipids with identical chain lengths but different headgroups (Struppe et al., 2000).

One important role of the lipid bilayer is that it shields the hydrophobic residues of a transmembrane domain from exposure to solvent water molecules. Of particular interest is determining the residues that are located at the boundary interface between the lipid core and the headgroup region of the bilayer. Although Demmers et al used mass spectrometry to assign the slowly exchanging amides to the hydrophobic core region of a transmembrane peptide, mass spectrometry currently does not allow for site specific information to be obtained (Demmers et al., 2000). On the other hand, NMR can provide information about the amide exchange of individual residues from amide-water chemical exchange cross-peaks in NOESY spectra at neutral pH (Gemmecker et al., 1993; Mori et al., 1997). One goal of this work is to analyze the chemical exchange of individual residues in a model transmembrane peptide incorporated in unaligned bicelles.

A second important role of the lipid bilayer is that it may aid in the formation of secondary and tertiary structure through peptide-lipid contacts. Amide-lipid NOEs have been observed for peptides in micellar

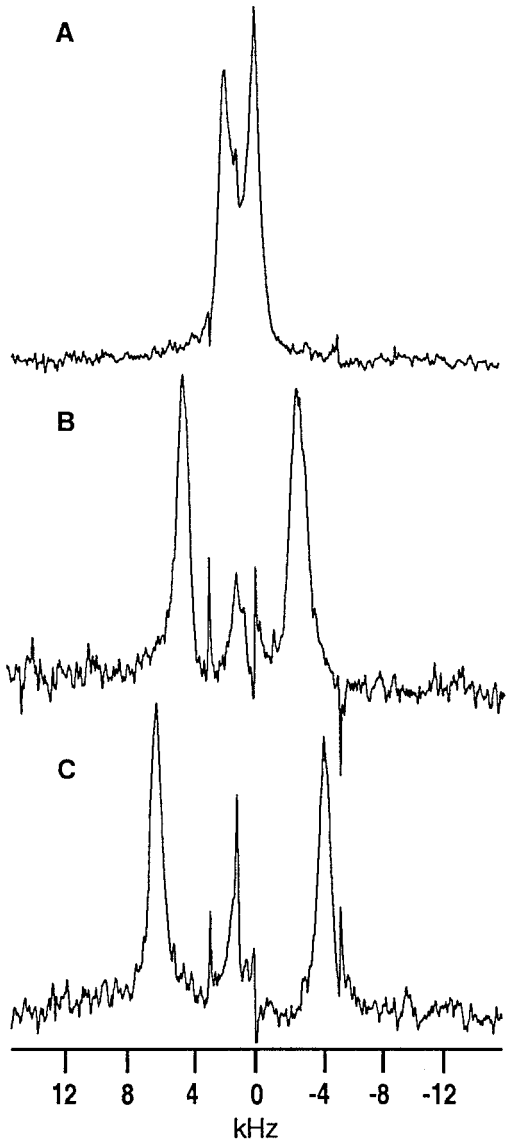

Figure 2. Quadrupolar splittings of P16 in aligned bicelles. (A) A7-d_3. (B) A12-d_3. (C) A16-d_3.

solution, and give information about which residues are in contact with the lipids (Losonczi et al., 2000; Seigneuret, 1999; Williams et al., 1996). However, because micelles do not have a bilayer, interpretation of the NOEs in the context of a biological membrane is limited. Consequently, a second goal of this work was to analyze peptide-lipid NOEs of individual residues in a model transmembrane peptide embedded in the bilayer of a bicelle.

A significant amount of water permeates into the headgroup region of the bilayer, and consequently

amide-water chemical exchange alone may not be able to distinguish residues at the lipid-water interface from those in the bulk solution (White and Wimley, 1999). Magic angle spinning experiments on multilamellar vesicles have shown NOEs between the hydrocarbon tails and the choline headgroups (Huster and Gawrisch, 1999). Thus, amide-lipid NOEs alone may not be able to distinguish residues in the headgroup interface from those in the hydrophobic core. A third goal of this work was therefore to analyze both chemical exchange and amide-lipid NOEs simultaneously to accurately assign residues to the headgroup interface region. Others have used a combined approach of analyzing both amide-water chemical exchange and amide-lipid NOEs but the curvature of the micelles prevented any definitive conclusions of site-specific localization with respect to the hydrophobic core (Losonczi et al., 2000; Williams et al., 1996).

In this study we employed a model transmembrane peptide, P16 (Ac-KKGLLLALLLLALLLALLLKKA-NH_2), which is comprised of a sixteen amino acid leucine-rich hydrophobic stretch flanked by two pairs of lysine residues which serve as anchors (Webb et al., 1998). P16 derivatives have been shown to adopt a transbilayer configuration in lipid bilayers and in bicelles (Huschilt et al., 1989; Sanders and Landis, 1995). The P16 peptide was incorporated in small unaligned DMPC/DHPC bicelles (Glover et al., 2001a) and 2D NOESY experiments were collected. Band-selective NOESY experiments in which either one or both phospholipids were chain perdeuterated revealed that P16 was indeed interacting with the 'bilayered' region of the bicelles. ^{15}N-edited 2D NOESY experiments revealed amide-water chemical exchange cross-peaks of residues accessible to solvent water and amide-lipid NOEs of residues interacting with the lipid bilayer. A combined analysis facilitated the classification of each residue according to its position with respect to the lipid bilayer.

Material and methods

Materials

Dimyristoylphosphatidylcholine (DMPC), and dihexanoylphosphatidylcholine (DHPC) and their chain perdeuterated counterparts were purchased from Avanti Polar Lipids (Alabaster, AL). HPLC grade acetic acid and HEPES were purchased from Fisher Scientific (Pittsburgh, PA). HPLC grade 1-butanol was purchased from Aldrich Chemical Company (Milwakee, WI). Deuterium oxide and ^{15}N labeled amino acids were purchased from Cambridge Isotopes (Cambridge, MA).

Peptide preparation

P16 (Ac-KKGLLLALLLLALLLALLLKKA-NH_2) and P16W (Ac-KKGLLLALLLWALLLALLLKKA-NH_2) were prepared according to previous published methods (Glover et al., 1999). Crude peptide was purified by reverse phase high performance liquid chromatography using a Phenomenex Jupiter C4 column and a linear gradient from 80% water 20% acetic acid to 80% 1-butanol 20% acetic acid. Peptide purity was verified by MALDI-TOF mass spectrometry.

Sample preparation

Bicellar samples were prepared by dissolving the peptide and DMPC or DMPC-d_{54} in 1.4 ml of triflouroethanol (TFE). Next, the TFE was rapidly injected via syringe into 20 ml of water at 50°, and the resultant clear solution was frozen and lyophilized to dryness. Next, appropriate amounts of water (deuterium depleted water was used for solid state samples), D_2O (omitted in solid state samples), 25% (w/w) solution of DHPC or DHPC-d_{22} in water, and 1 M HEPES buffer pH 7.5 were added to the dry powder. Samples were vigorously vortexed and taken through several heating and cooling cycles until homogeneous and clear. For solution NMR samples, final concentrations of constituents in the samples were 15% (w/w) total lipid ($q = 0.5$), 5% (v/v) D_2O, 25 mM HEPES, and a 1:45 ratio of P16 to DMPC. For solid-state samples, final concentrations of constituents in the samples were 20% (w/w) total lipid ($q = 3.5$), 25 mM HEPES, and a 1:40 ratio of P16 to DMPC. Circular dichroism experiments were prepared by a 5-fold dilution with water of the corresponding solution NMR sample.

Solution NMR methods

All NMR experiments were run at 37 °C on a Bruker DRX-600 NMR spectrometer operating at a ^{1}H resonance frequency of 600 MHz and equipped with pulsed field x,y,z-gradients. All experiments were acquired with the ^{1}H carrier centered on the water resonance and the ^{15}N carrier set at 119 ppm. In all pulse sequences quadrature-detection for the indirectly detected dimension (t_1) was obtained using States-TPPI

Table 1. List of P16 peptides with selective ^{15}N labeling

Version	Sequence[a]
1	Ac-K K **G** **L** L L A L L L L **A** L L L A L **L** L K K **A**-NH_2
2	Ac-K K G L **L** L A L L L L A L L L **A** **L** L L K K A-NH_2
3	Ac-K K G L L **L** **A** L L L L A L L L A L L **L** K K A-NH_2

[a]Boxes denote residues which were ^{15}N labeled.

(Marion et al., 1989). In all experiments an inter-scan repetition delay of 2 s was used to allow for the recovery of the lipid and water magnetizations. The band-selective NOESY experiments were acquired as a data matrix of 128* (t_1) × 512* (t_2) complex points, with $t_{1,max} = 14.23$ ms and $t_{2,max} = 56.93$ ms. A total of 80 scans were accumulated per serial file. The NOE mixing time had a total duration of 90 ms (Huster and Gawrisch, 1999), and a non-selective 180° ^1H pulse was inserted in the middle of the mixing time. The water and lipid magnetizations were suppressed after the NOE mixing period and prior to acquisition by a double band-selective pulsed filed gradient spin-echo (Dalvit, 1998). A phase-modulated 1.8 ms REBURP pulse (Geen and Freeman, 1991) was used for selection of a frequency band centered at 3.10 ppm, and including both the water and the lipid resonances. The gradients for both spin-echos were at the magic angle (Mattiello et al., 1996) and the ratio between the strengths of the gradients in the first and second spin-echo was 1.89. All gradients in the spin-echo had a duration of 0.5 ms and the shape of the center lobe of the sin(x)/x function. The FHSQC (Mori et al., 1995) experiments were acquired with 16 scans as a data matrix of 64* (t_1) × 512* (t_2) complex points, with $t_{1,max} = 10.52$ ms and $t_{2,max} = 61.03$ ms. The 2D-NOESY-FHSQC experiments were acquired without incrementing the t_2 delay and with a 180° ^{15}N refocusing pulse inserted in the middle of t_2 thus avoiding ^{15}N frequency labeling. For the 2D-NOESY-FHSQC, 128 scans were recorded with a mixing time of 90 ms and the data matrix had 128* (t_1) × 512* (t_3) complex points, with $t_{1,max} = 18.28$ ms and $t_{3,max} = 61.03$ ms. Data sets were processed using Felix 97.0 (Molecular Simulations, San Diego, CA) with a 90° shifted squared sinebell apodization and zero filling by a factor of two, prior to Fourier transform and phase-correction. Previous work has shown that high quality HSQC–based spectra can be obtained for peptides associated tightly with unaligned bicelles (Glover et al., 2001b; Whiles et al., 2001). This is likely due to the high degree of motion of the lipid molecules (Vold et al., 1997).

Solid-state NMR methods

Deuterium quadrupole echo spectra were acquired at 55.3 MHz using a Chemagnetics CMX-250/360 spectrometer as previously described (Whiles et al., 2001). Data processing included fractional left shifting, zero filling, and multiplication by an exponential (25 and 500 Hz line broadening for lipid and peptide spectra respectively) of the second half of the quadrupole echo prior to Fourier transformation. The quadrupolar splittings of alanine-d_3 at three different positions in the peptide were analyzed to solve for the peptide tilt and its rotation about the helical axis (Jones et al., 1998). A C++ computer program allowed computation of the tilt angles (varied in 1° intervals from 0° to 90°) and the rotation angles (varied in 1° increments from 0° to 360°) that were consistent with the quadrupolar splitting of all three alanine labels. The program then ranked all possible tilt and rotation angle combinations based on the deviation of the quadrupolar splittings from the theoretical values for a particular tilt and rotation (Whiles et al., 2001).

Circular Dichroism spectroscopy

Circular Dichroism spectra were obtained at 37 °C on an Aviv Circular Dichroism Spectrometer Model 202.

Results and discussion

P16 (Ac-KKGLLLALLLLALLLALLLKKA-NH_2) has a high degree of chemical shift degeneracy for both ^1H and ^{15}N nuclei. Consequently, three versions of P16 were necessary, each with selective ^{15}N labeling, to unambiguously assign the residues (Table 1). The presence of strong H^NH^N(i, i+1) NOEs (Table 2) along with the circular dichroism spectrum of P16 (Figure 1), which showed the typical minima

Table 2. Summary of chemical shifts, NN(i, i+1) NOEs, amide-water exchange, amide-lipid NOEs, and residue classes of P16 in bicelles

Residue	**K**	**K**	**G**	**L**	**L**	**L**	**A**	**L**	**L**	**L**	**L**	**A**	**L**	**L**	**L**	**A**	**L**	**L**	**L**	**K**	**K**	**A**	**NH_2**
Chemical shift (ppm)			8.45	8.01	8.15	8.14	8.26					8.50				8.43	8.15	8.30	8.43			8.10	7.28, 7.10[a]
NN(i, i+1)[b]			—	—	—	—										—	—	—				—	
Amide-water exchange[c,d]			Y	N	N	N	N					N				N	N	N	N			Y	Y
Amide-lipid NOE[c,e]			Y	Y	Y	Y	Y					Y				Y	Y	Y	Y			Y	N
Class[f]	(II)	(II)	II	III	III	III	III	III	III	III	III	III	III	III	III	III	III	III	III	(II)	(II)	II	I

[a]The unlabeled C-terminal amide was observed in the band selective NOESY experiment.
[b]Selective labeling only allowed for observation of NN(i, i+1) NOEs.
[c]Y = Yes, presence of peak; N = No, absence of peak.
[d]Cross peak observed between amide and water (4.70 ppm) resonances.
[e]Cross peak observed between amide and lipid methylenes (1.31 ppm) resonances.
[f]Parentheses denote classifications that are likely but not unambiguously determined.

at 208 nm and 222 nm, indicated that P16 is highly α-helical.

To confirm the transbilayer orientation of P16, solid-state deuterium NMR in aligned bicelles was carried out on three separately labeled peptides (A7-d_3, A12-d_3, A16-d_3) (Jones et al., 1998; Whiles et al., 2001). Preliminary solid-state ^{2}H lipid spectra of both chain perdeuterated DMPC and DHPC confirmed that the bicelles remained well aligned and stable in the presence of peptide. The quadrupolar splittings obtained for the three peptides (Figure 2, Table 3) were analyzed as previously described by Whiles et al. and the resulting tilt angle was 33–35 deg with respect to the bicelle normal. This agrees well with the 25 ± 10 deg with respect to the bicelle normal obtained for a similar P16 peptide in lipid bilayers using X-ray methods (Huschilt et al., 1989) and in aligned bicelles using ^{13}C chemical shift anisotropy (Sanders and Landis, 1995). These observations are consistent with a membrane spanning orientation for P16.

Several band selective 2D-NOESY spectra, acquired in bicellar solutions prepared with three combinations of deuterated and protonated DMPC and DHPC, allowed us to disentangle the NOEs due to amide-peptide, amide-DHPC and amide-DMPC interactions thus probing where in the bicelle (rim *vs.* planar region) P16 is located (Figure 3). A band selective NOESY is advantageous for bicellar solutions because it suppresses the strong lipid resonances in the upfield region of the directly acquired dimension, while leaving the amide resonances unaffected (Seigneuret and Levy, 1995). Since, this suppression is not applied in the indirectly dectected dimension, NOEs between the peptide amides and the lipids are readily observed. In this study, peptide-lipid NOEs were ascertained at 1.31 ppm, which corresponds to the resonance frequency of the majority of the methylene protons in the lipid chains (Huster et al., 1999). Strong NOEs between the amides and DMPC showed that the P16 peptide interacts with the planar region (Figure 3C), as opposed to the lack of significant NOEs between amides and DHPC (amide-rim) (Figure 3B).

Table 3. Quadrupolar splittings in aligned bicelles

Residue	P16 splitting (kHz)	P16W splitting (kHz)
A7	1.6 ± 1.0	7.6 ± 1.0
A12	7.1 ± 1.0	12.7 ± 1.0
A16	10.3 ± 1.0	13.6 ± 1.0

For comparison, a slightly different version of P16, P16W (Ac-KKGLLLALLLWALLLALLLKKA-NH_2) was prepared on the rationale that the tryptophan might promote a surface orientation (Yau et al., 1998). This peptide gave very different quadrupolar splittings (Table 3) consistent with a parallel orientation with respect to the plane of the bicelles (72–82 deg with respect to the bicelle normal). Unlike P16, P16W showed NOEs to both the DMPC and DHPC (Figure 4) confirming that P16W associates with the bicelle differently from P16. Thus, despite the rapid exchange of the DHPC between bicelle and solution (Glover et al., 2001a), peptide-DHPC NOEs can be observed. This result reinforces the conclusion that P16 is associated primarily with the planar region of the bicelle, which is the more biologically relevant portion.

Next, both amide-lipid NOEs and amide-water chemical exchange cross-peaks were evaluated for each labeled residue (Figure 5, Table 2). For example in P16 version one, residues L4, A12, and

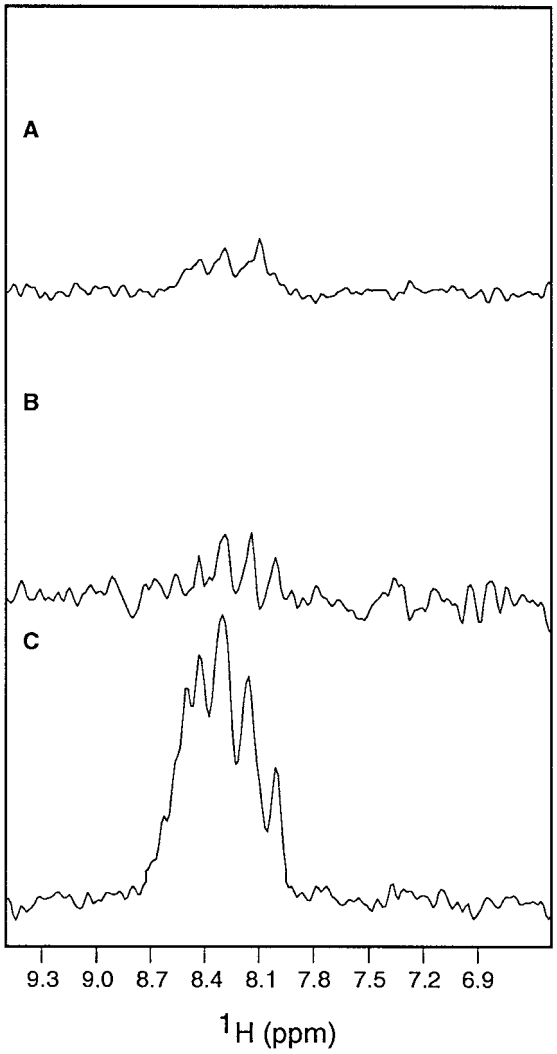

Figure 3. One-dimensional horizontal slices taken at 1.31 ppm (resonance frequency that contains contributions from the methylene protons of the lipid chains) from various band-selective NOESY spectra of P16 in unaligned bicelles with different deuteration schemes. (A) Bicelles prepared with DMPC-d_{54}/DHPC-d_{22} (amide-peptide cross-peaks). (B) Bicelles prepared with DMPC-d_{54}/DHPC (amide-rim cross-peaks, spectrum acquired with 2.88 times as many scans to equalize the intensity discrepancy arising from differences in the number of methylenes between DMPC and DHPC as well as differences in the concentrations of the two lipids (two times as much DHPC as DMPC)). (C) Bicelles prepared with DMPC/DHPC-d_{22} (amide-planar region cross-peaks). Spectrum **A** was subtracted from spectra (B) and (C) to eliminate contributions from amide-peptide cross-peaks.

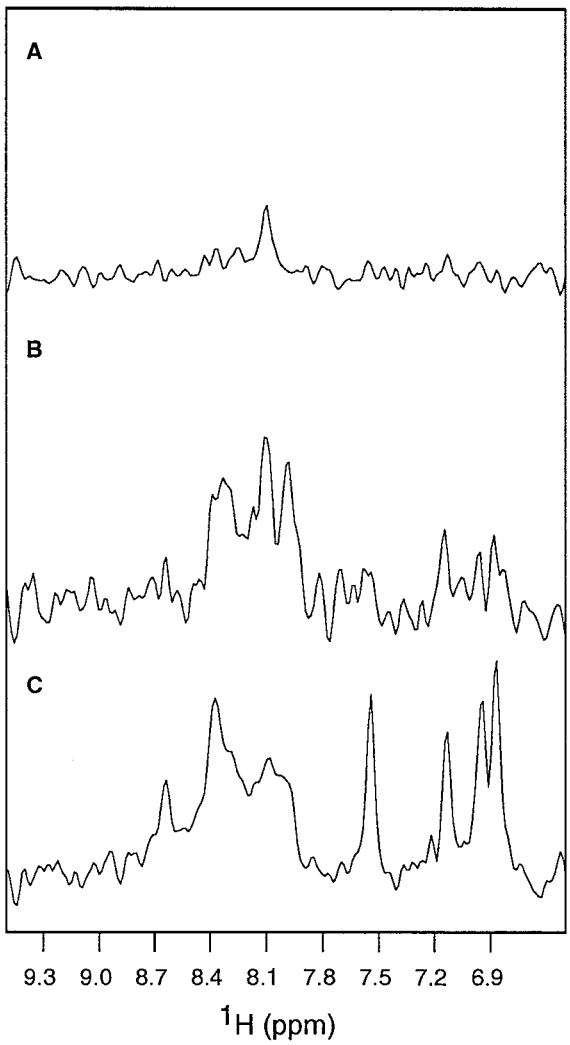

Figure 4. One-dimensional horizontal slices from various band-selective NOESY spectra of P16W in unaligned bicelles. (A), (B) and (C) are as in Figure 3.

L18 showed an amide-lipid NOE, and no amide-water chemical exchange cross-peaks, while residues G3 and A22 showed both amide-lipid NOEs and amide-water chemical exchange cross-peaks (Figure 5). The C-terminal amide showed chemical exchange to water and no NOEs to the lipids. The absence of an amide-lipid NOE for the C-terminal amide is not caused by fast dynamics, because the NOE from H^N A22 to the C-terminal amide is readily observed. Similar analyses were peformed for P16 versions 2 and 3 and the results are summarized in Table 2.

The amide-water chemical exchange and amide-lipid NOE data in Table 2 reveal the presence of three classes of residues (Figure 6): Class I represents

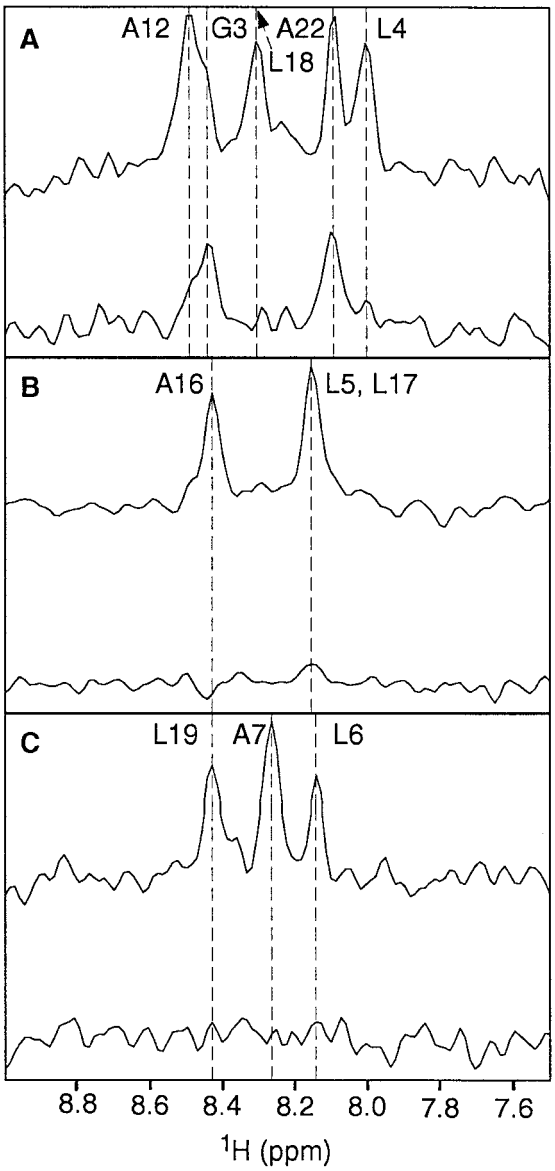

Figure 5. One-dimensional horizontal slices taken from a ^{15}N NOESY spectrum of P16 in unaligned bicelles. The top spectra in each panel was taken at the lipid methylene resonance (1.31 ppm). The bottom spectra in each panel was taken at the water resonance (4.70 ppm). (A) Version 1. (B) Version 2. (C) Version 3.

residues which show amide-water chemical exchange cross peaks but no amide-lipid NOE cross peaks, and corresponds to those residues that are in contact with bulk water molecules and lie outside both the DMPC hydrophobic core and the headgroup region. Class II comprises those residues in which both amide-water chemical exchange and peptide-lipid NOEs are observed. These are residues that lie in the headgroup region. Class III represents residues that had amide-lipid NOEs but no chemical exchange with water. These are residues that are embedded in the hydrophobic core of the lipid bilayer.

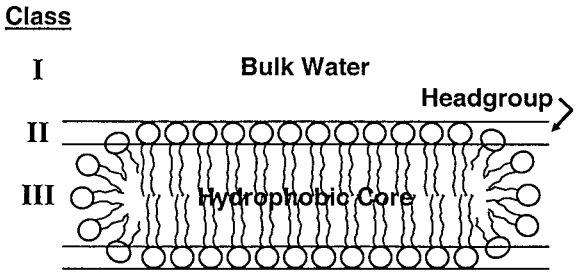

Figure 6. Diagram of a cross section of a bicelle showing the location of the three classes of residues.

The assignment of residues L4, L5, L6, A7, A12, A16, L17, L18, and L19 to Class III (Table 2) allowed us to additionally classify all the residues between L4 and L19 to Class III. Thus, the entire central region of the P16 peptide resides in the hydrophobic core of the membrane. Residue A22 was assigned to Class II while L19 was assigned to Class III. This left K20 and K21 as either being Class II or Class III, and we suggest the probable assignment of these residues to Class II because they are charged. G3 was assigned to Class II, and therefore K1 and K2 could be Class II or Class I. Again based on charge their probable assignment is Class II.

Conclusions

We have shown that the transmembrane peptide, P16, spans the planar region of small unaligned bicelles because it has a transmembrane orientation and interacts primarily with the long chain lipids of the bicelle rather than with the rim. Sixteen residues, all in the central portion of the P16 peptide were assigned to Class III. Flanking these on either side were three residues that were assigned to Class II. The C-terminal amide was assigned to Class I. These assignments are fully consistent with an α-helical structure spanning the membrane. First of all, the sixteen residues assigned to the hydrophobic core of the membrane span a predicted helix length of 24.8 Å which matches closely with the length of the hydrophobic core of a DMPC bilayer (22.8 Å) (Sperotto and Mouritsen, 1988). Second, the three residues on either side of the membrane which were assigned to Class II comprise approximately one turn of the helix, which is the min-

imum peptide length required to span the headgroup region. These residues interact with both the lipid and the solvent water molecules and precisely define the membrane water interface with respect to a transmembrane segment. Taken together, chemical exchange data and amide-lipid NOEs thus provide a robust dataset upon which to assign the location of individual residues within bilayers. Furthermore, they show that bicelles are a biologically relevant membrane mimetic for the study of bilayer–peptide interactions.

Acknowledgements

We thank Dr Susan Taylor for use of her circular dichroism spectrometer, Dr Elizabeth Komives for use of her mass spectrometer and useful discussions, and Dr John Wright for NMR assistance. This work was supported by NIH (5 R01 GM54034) grants to Regitze R. Vold. K.J.G. was supported by the NIH Heme & Blood Proteins Training Grant.

References

Arora, A., Abildgaard, F., Bushweller, J.H. and Tamm, L.K. (2001) *Nat. Struct. Biol.*, **8**, 334–338.

Cross, T.A. and Opella, S.J. (1994) *Curr. Opin. Struct. Biol.*, **4**, 574–581.

Czerski, L. and Sanders, C.R. (2000) *Anal. Biochem.*, **284**, 327–333.

Dalvit, C. (1998) *J. Biomol. NMR*, **11**, 437–444.

Demmers, J.A.A., Haverkamp, J., Heck, A.J.R., Koeppe II, R.E. and Killian, J.A. (2000) *Proc. Natl. Acad. Sci. USA*, **97**, 3189–3194.

Geen, H. and Freeman, R.J. (1991) *J. Magn. Reson.*, **93**, 93–141.

Gemmecker, G., Jahnke, W. and Kessler, H. (1993) *J. Am. Chem. Soc.*, **115**, 11620–11621.

Glover, K.J., Martini, P.M., Vold, R.R. and Komives, E.A. (1999) *Anal. Biochem.*, **272**, 270–274.

Glover, K.J., Whiles, J.A., Wu, G., Yu, N., Deems, R., Struppe, J.O., Stark, R.E., Komives, E.A. and Vold, R.R. (2001a) *Biophys. J.*, **81**, 2163–2171.

Glover, K.J., Whiles, J.A., Wood, M.J., Melacini, G., Komives, E.A. and Vold, R.R. (2001b) *Biochemistry*, in press.

Huschilt, J.C., Millman, B.M. and Davis, J.H. (1989) *Biochim. Biophys. Acta*, **979**, 139–141.

Huster, D. and Gawrisch, K. (1999) *J. Am. Chem. Soc.*, **121**, 1992–1993.

Huster, D., Arnold, K. and Gawrisch, K. (1999) *J. Phys. Chem. B.*, **103**, 243–251.

Jones, D.H., Barber, K.R., VanDerLoo, E.W. and Grant, C.W.M. (1998) *Biochemistry*, **37**, 16780–16787.

Kallick, D.B. (1993) *J. Am. Chem. Soc.*, **115**, 9317–9318.

Losonczi, J.A., Olejniczak, E.T., Betz, S.F., Harlan, J.E., Mack, J. and Fesik, S.W. (2000) *Biochemistry*, **39**, 11024–11033.

MacKenzie, K.R., Prestegard, J.H. and Engelman, D.M. (1997) *Science*, **276**, 131–133.

Marion, D., Ikura, M., Tschudin, R. and Bax, A. (1989) *J. Magn. Reson.*, **85**, 393–399.

Mattiello, D.l., Warren, W.S., Mueller, L. and Farmer, B.T. (1996) *J. Am. Chem. Soc.*, **118**, 3253–3261.

Mori, S., Abeygunawardana, C., Berg, J.M. and Van Zijl, P.C.M. (1997) *J. Am. Chem. Soc.*, **119**, 6844–6852.

Mori, S., Abeygunawardana, C., Johnson, M.O. and Van Zijl, P.C.M. (1995) *J. Magn. Reson. Series B*, **108**, 94–98.

Mumm, J.S. and Kopan, R. (2000) *Dev. Biol.*, **228**, 151–165.

Opella, S.J. (1997) *Nat. Struct. Biol.*, **Suppl.**, 845–848.

Ram, P. and Prestegard, J.H. (1988) *Biochim. Biophys. Acta*, **940**, 289–294.

Sanders, C.R. and Landis, G.C. (1995) *Biochemistry*, **43**, 4030–4040.

Sanders, C.R. and Prestegard, J.H. (1990) *Biophys. J.*, **58**, 447–460.

Sanders, C.R. and Schwonek, J.P. (1992) *Biochemistry*, **31**, 8898–8905.

Sanders, C.R., Hare, B.J., Howard, K.P. and Prestegard, J.H. (1994) *Progr. NMR Spectr.*, **26**, 421–444.

Sanders, C.R., Schaff, J.E. and Prestegard, J.H. (1993) *Biophys. J.*, **64**, 1069–1080.

Seigneuret, M. (1999) *J. Biomol. NMR*, **13**, 31–41.

Seigneuret, M. and Levy, D. (1995) *J. Biomol. NMR*, **5**, 345–352.

Sperotto, M.M. and Mouritsen, O.G. (1988) *Eur. Biophys. J.*, **16**, 1–10.

Struppe, J.O., Whiles, J.A. and Vold, R.R. (2000) *Biophys. J.*, **78**, 281–289.

Vold, R.R., Prosser, R.S. and Deese, A.J. (1997) *J. Biomol. NMR*, **9**, 329–335.

Webb, R.J., East, J.M., Sharma, R.P. and Lee, A.G. (1998) *Biochemistry*, **37**, 673–679.

Whiles, J.A., Brasseur, R., Glover, K.J., Melacini, G., Komives, E.A. and Vold, R.R. (2001) *Biophys. J.*, **80**, 280–293.

White, S.H. and Wimley, W.C. (1999) *Annu. Rev. Biophys. Biomol. Struct.*, **28**, 319–365.

Williams, K.A., Farrow, N.A., Deber, C.M. and Kay, L.E. (1996) *Biochemistry*, **35**, 5145–5157.

Yau, W.-M., Wimley, W.C., Gawrisch, K. and White, S.H. (1998) *Biochemistry*, **37**, 14713–14718.